White Rose Research Online

eprints@whiterose.ac.uk
https://eprints.whiterose.ac.uk
Universities of Leeds, Sheffield and York

Deposited via The University of Leeds.

White Rose Research Online URL for this paper:
https://eprints.whiterose.ac.uk/id/eprint/104485/

Version: Accepted Version

Article:
Gregory, RC, Hemsworth, GR, Turkenburg, JP et al. (2016) Activity, stability and 3-D structure of the Cu(II) form of a chitin-active lytic polysaccharide monooxygenase from Bacillus amyloliquefaciens. Dalton Transactions, 45 (42). pp. 16904-16912. ISSN: 1477-9226

https://doi.org/10.1039/C6DT02793H

© 2016, Royal Society of Chemistry. This is an author produced version of a paper published in Dalton Transactions. Uploaded in accordance with the publisher's self-archiving policy.

Reuse
Items deposited in White Rose Research Online are protected by copyright, with all rights reserved unless indicated otherwise. They may be downloaded and/or printed for private study, or other acts as permitted by national copyright laws. The publisher or other rights holders may allow further reproduction and re-use of the full text version. This is indicated by the licence information on the White Rose Research Online record for the item.

Takedown
If you consider content in White Rose Research Online to be in breach of UK law, please notify us by emailing eprints@whiterose.ac.uk including the URL of the record and the reason for the withdrawal request.

UNIVERSITY OF LEEDS
University of Sheffield
UNIVERSITY of York

Please do not adjust margins
View Article Online
DOI: 10.1039/C6DT02793H

Journal Name

ARTICLE

Published on 07 September 2016. Downloaded by University of Leeds on 07/09/2016 14:17:33.

Activity, stability and 3-D structure of the Cu(II) form of a chitin-active lytic polysaccharide monooxygenase from *Bacillus amyloliquefaciens*

Received 00th January 20xx,
Accepted 00th January 20xx

DOI: 10.1039/x0xx00000x

www.rsc.org/

Rebecca C Gregory[a], Glyn R Hemsworth[a], Johan P Turkenburg[a], Samuel J Hart[a], Paul H Walton[b] and Gideon J Davies[a†]

The enzymatic deconstruction of recalcitrant polysaccharide biomass is central to the conversion of these substrates for societal benefit, such as in biofuels. Traditional models for enzyme-catalysed polysaccharide degradation involved the synergistic action of *endo*-, *exo*-and processive glycoside hydrolases working in concert to hydrolyse the substrate. More recently this model has been succeeded by one featuring a newly discovered class of mononuclear copper enzymes: lytic polysaccharide monooxygenases (LPMOs; classified as Auxiliary Activity (AA) enzymes in the CAZy classification). In 2013, the structure of an LPMO from *Bacillus amyloliquefaciens*, *Ba*AA10, was solved with the Cu centre photoreduced to Cu(I) in the X-ray beam. Here we present the catalytic activity of *Ba*AA10. We show that it is a chitin-active LPMO, active on both α and β chitin, with the Cu(II) binding with low nM K_D, and the substrate greatly increasing the thermal stability of the enzyme. A spiral data collection strategy has been used to facilitate access to the previously unobservable Cu(II) state of the active centre, revealing a coordination geometry around the copper which is distorted from axial symmetry, consistent with the previous findings from EPR spectroscopy.

Introduction

Biofuel production from abundant polysaccharides is an important area of research, key to which is the development of efficient enzymatic methods which can overcome the chemical and physical recalcitrance of cellulose and chitin[1]. Traditionally, enzymatic degradation of polysaccharides was thought to occur through the synergistic action of classical glycoside hydrolases to generate oligosaccharides that could then be converted to soluble sugars and fermented to ethanol. β-linked polysaccharides such as cellulose (a β-1,4-linked polymer of glucose) and chitin (a β-1,4-linked polymer of *N*-acetyl glucosamine) are, however, very highly resistant to degradation such that classical hydrolase action is slow and inefficient[2]. The recalcitrance of these substrates is linked to their highly crystalline structures in which there are few access points for canonical cellulases/chitinases and also linked to the low level of synergy between *endo*- and *exo*-enzymes (reviewed, for example in Horn *et al*[2]).

A newly discovered class of enzymes has recently overturned the traditional understanding of biomass degradation and thus offers new hope for viable production of biofuels. These enzymes are the *lytic polysaccharide monooxygenases* (LPMOs), which are currently sequence-classified into four families in the CAZy database (www.CAZy.org) - AA9 and AA10 (previously GH61 and CBM33 respectively)[3], as well as the more recent AA11[4] and AA13[5, 6]. These fascinating enzymes have had a significant impact not only on our understanding of biological biomass degradation but also on commercial biofuel production. Accordingly, LPMOs have been at the centre of much research attention, with several recent reviews providing insights into the published data and the possible mechanisms of action of LPMOs[7-11], including a very recent structure of an LPMO in association with an oligosaccharide substrate [12]. LPMOs use an oxidative mechanism to introduce chain breaks into polysaccharides thereby augmenting the activity of classical glycoside hydrolases, as shown by Vaaje Kolstad *et al*[13] in their breakthrough study of CBP21 (chitin-binding protein 21) from *Serratia marcescens.* Using a copper co-factor together with an electron source which can be a small-molecule reducing agent, such as ascorbate[14], or a protein partner such as cellobiose dehydrogenase (CDH) in fungi[15-17], LPMOs introduce a single atom from O_2 at either the C1 or C4 position of the sugar ring, destabilising the glycoside linkage resulting in chain cleavage[2, 14-16, 18]. The strength of the scissile C-H bond which has been estimated to be ca 95 kcal/mol, indicative of the powerful oxidative nature of LPMOs. C1-oxidised products are characterised by an aldonic acid at their reducing-end resulting from the hydration of the lactone produced by LPMO action,

[a] *Structural Biology Laboratory, University of York, Heslington, York, YO10 5DD, United Kingdom.*
[b] *Department of Chemistry, University of York, Heslington, York, YO10 5DD, United Kingdom.*
† To whom correspondence may be addressed: gideon.davies@york.ac.uk
Electronic Supplementary Information (ESI) available: See DOI: 10.1039/x0xx00000x

Dalton Transactions Accepted Manuscript

Please do not adjust margins

View Article Online
DOI: 10.1039/C6DT02793H

Published on 07 September 2016. Downloaded by University of Leeds on 07/09/2016 14:17:33.

whilst C4-oxidation results in non-reducing-end ketoaldose products[18]. Interestingly, most AA10s produce predominantly even-numbered oligosaccharide products (i.e. with degrees of polymerisation = 2, 4, 6 etc.)[13, 19, 20], whilst fungal enzymes produce a range of products with both odd and even-numbered degrees of polymerisation[14, 21, 22].

Studies into the likely mechanism of action used by LPMOs have centred on understanding their copper active site geometries[7-9, 23-25]. All LPMOs characterised to date bind a single copper ion in their active sites via the "histidine brace"[14] (Figure 1) This unusual arrangement makes use of the amino-terminus and side-chain of the N-terminal histidine to directly coordinate copper together with a second histidine side-chain in a T-shaped geometry. A similar coordination geometry is observed at the active site of particulate methane monooxygenase, albeit in this enzyme as part of the coordination of two copper ions, the nuclearity of which however is an area of current debate. For AA9 LPMOs the equatorial plane around the Cu(II) ion is typically completed by coordination from a water/hydroxide molecule, with longer axial interactions provided by an additional water molecule and often the OH group of a tyrosine. For AA10 LPMOs the copper coordination sphere is completed by two water molecules, both of which do not sit in the equatorial plane created by the protein-derived ligands[26]. Computational methods have recently probed the mechanism of reaction used by AA9s [23, 27]. Kjaergaard et al used density functional theory (DFT) calculations, augmented with experimental data from EXAFS and XANES spectroscopies which suggested that, in the absence of substrate, a thermodynamically plausible oxygen species is an end-on triplet Cu-AA9-superoxide generated by the one electron reduction of O_2, which could be the oxidative species which carries out the attack of the C-H bond in the substrate In contrast, in a purely computational approach, Kim et al modelled two possible reaction mechanisms in the presence of substrate, which suggested that the more powerful Cu(II)-oxyl species was necessary to hydroxylate the substrate[28], although it is notable in these calculations that the oxyl needs to be placed in the axial position of the Jahn-Teller distorted copper coordination sphere for it to be able to react with the substrate.

Given the role in biofuel production, a process dominated by fungal enzymes, much of the research focus on LPMOs has been placed on fungal enzymes and their action on cellulose. Bacterial enzymes are also able to boost the activity of classical glycoside hydrolases. A recent study of an AA10 from *Streptomyces griseus*, for example, has shown 30- and 20-fold improvements in the degradation of α- and β-chitin, respectively, by chitinases after the addition of the LPMO[29]. Several studies have now shown that chitin-active AA10s appear to display distinct active site geometries to those observed for other LPMOs [26, 30, 31].

In previous work, we presented the structural and spectroscopic characterisation of a bacterial AA10 LPMO from the *Bacillus amyloliquefaciens*, *Ba*AA10[32]. In our structural analysis we found that the active site copper had been reduced to Cu(I) in the X-ray beam, and observed similar rapid photoreduction of copper using XANES on the enzyme in solution[32]. X-band electron paramagnetic resonance (EPR) spectroscopy afforded a highly rhombic spectrum with a reduced Az value, a likely explanation of which was that the $d(x^2-y^2)$ SOMO has significant $d(z^2)$ mixing, demonstrating that the coordination at the copper was significantly distorted from an axial geometry[32].

Here we present an improved over-expression procedure for *Ba*AA10 using an N-terminal SUMO fusion construct. Expressed intracellularly, following SUMO protease treatment, active *Ba*AA10 was produced in greater yields than obtained via secretion to the periplasm. Originally identified as a chitin binding protein (ChbB)[33], which could bind to both α and β forms of chitin, we now show that *Ba*AA10 is a chitin-active LPMO primarily releasing predominantly even-numbered products from both α and β chitin; consistent with reports of other chitin-active LPMOs. Furthermore, using a spiral data collection technique, we have determined a structure of the enzyme with its active site cofactor in the Cu(II) state confirming the active site geometry determined previously for this protein from EPR studies, and further supporting wider findings that chitin-active AA10s display a Cu(II) coordination geometry which is distorted from axial symmetry.

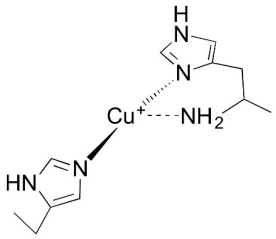

Figure 1. Schematic representation of the histidine brace LPMO active site.

Results and Discussion

Improved over-expression of *Ba*AA10 using an intracellular SUMO construct

One of the major difficulties in producing LPMOs is their requirement for an N-terminal histidine in the mature protein, with the amino terminus forming an integral part of the active site. In our previous work, recombinant *Ba*AA10 was secreted into the periplasm of *E. coli*, giving yields of ~3-4 mg protein per litre of culture[32]. We reasoned that the protein yield could be improved by avoiding protein secretion into the periplasm and including an affinity tag to simplify the protein purification. An improved expression and purification protocol was therefore obtained by cloning the *Ba*AA10 gene into the Champion pET-SUMO vector (Figure S1A). When expressed in BL21*(DE3) cells we were able to express *Ba*AA10 in the cytoplasm, obtaining significantly higher protein expression yields, and simplifying the protein purification by using nickel affinity chromatography. The structure specific SUMO protease cleaved the enzyme adjacent to the active site histidine, yielding high purity *Ba*AA10 with yields in excess of 9 mg of protein per litre of culture (Figure S1B).

Dalton Transactions Accepted Manuscript

This journal is © The Royal Society of Chemistry 20xx

Please do not adjust margins
View Article Online
DOI: 10.1039/C6DT02793H

Published on 07 September 2016. Downloaded by University of Leeds on 07/09/2016 14:17:33.

Cu binding to BaAA10 by displacement ITC

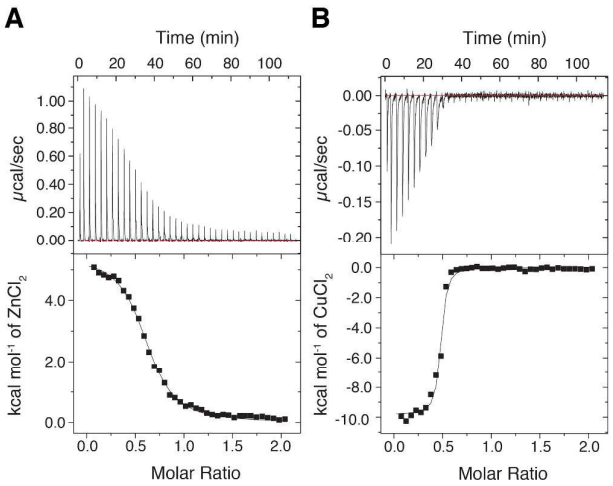

Figure 2. (A) Isothermal titration calorimetry (ITC) plot of Zn^{2+} binding to *Ba*AA10 at pH 5, to obtain parameters to be used for the Cu^{2+} displacement reaction. The concentration of the protein (*Ba*AA10) inside the cell was 200 µM and the concentration of $ZnCl_2$ was 2 mM. **(B)** The Cu^{2+} displacement result carried out at pH5, whereby the concentration of $Cu(II)Cl_2$ titrated into the cell was 500 µM.

Having improved the protein purification method for *Ba*AA10, we sought to confirm that the protein behaved as the periplasmically produced protein had in solution. It has previously been shown that binding of copper to LPMOs is extremely strong, with dissociation constants (K_D) on the nM scale. The published K_D for *Ba*AA10 (then *Ba*CBM33) is 6 nM at pH 5[32], with another LPMO (CBP21) having a K_D reported at 55 nM[19]. Using ITC we were able to confirm that the SUMO purified protein bound copper(II) with high affinity as seen previously (data not shown). We took this analysis further using displacement ITC to obtain a more accurate binding constant for Cu^{2+} binding to *Ba*AA10. This method relies on using a weaker binding metal, Zn^{2+} in this case, to bind to the protein, which can then be displaced using the high affinity metal (Cu^{2+}) to obtain a more accurate measure of copper binding[4]. Using this approach the K_D for Zn^{2+} binding at pH 5 was determined to be 8.1 µM (Figure 2A). The subsequent competitive binding titration, displacing the Zn^{2+} with Cu^{2+}, produced results that yielded a K_D for Cu^{2+} binding of 43 nM ± 2 nM at pH 5, with a reliability value (χ^2) of 8.78 (Figure 2B). The stoichiometry obtained during these analyses came out at ~0.5 rather than 1. This is not uncommon for these enzymes given their high affinity for copper which is very hard to remove from glassware and buffers and is scavenged rapidly by the enzyme, making it very challenging to completely demetallate LPMOs. This should not have much influence on the measured K_D as seen here, as the obtained values match closely to those published for other enzymes in this family[31, 32, 34].

Substrate Binding to BaAA10

Previous work has shown that *Ba*AA10 is a chitin binding protein[33]. To probe further the potential range of substrates with which *Ba*AA10 might interact, the thermal stability of the enzyme in the presence of poly- and oligosaccharides was investigated using differential scanning fluorimetry. Figure 3A shows that there is a clear increase in stability of the enzyme in the presence of chitin, giving a ΔT_m of 8.3 °C compared to the native enzyme. Experiments carried out using cellulose (Avicel) and chitohexaose as other potential substrates show no significant change in melting temperature, indicating that only chitin binds significantly and thus is the most likely candidate as the *Ba*AA10 substrate. Most notably, a soluble chitin-derived hexasaccharide, chitohexaose, had no measurable effect on stability, showing that it is the crystalline polymer alone that is the substrate. Chitin in the absence of enzyme was also tested (result not shown) to see if it interfered with the fluorescence readings. However, no melting curve was obtained showing that any change in dissociation could solely be credited to the enzyme-substrate complex. A control sample carried out in the presence of EDTA provides a similar result as the native enzyme, with only a 1.8 degree decrease in melting temperature.

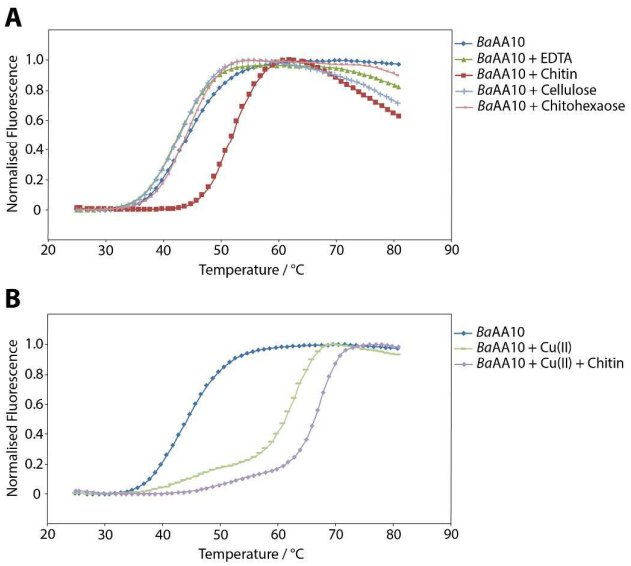

Figure 3. Denaturation curves displaying the normalised fluorescence against temperature for: **(A)** *Ba*AA10 with a variety of ligands including EDTA, chitin, cellulose and chitohexaose, and **(B)** *Ba*AA10 with copper and chitin as the substrate. The corresponding melting temperatures (T_m) determined in analysis were: *Ba*AA10 = 43.6 ºC, *Ba*AA10 + EDTA = 41.8 ºC, *Ba*AA10 + Chitin = 51.9 ºC, *Ba*AA10 + Cellulose = 42.9 ºC, and *Ba*AA10 + Chitohexaose = 44.2 ºC, *Ba*AA10 + Cu^{2+} = 65.2 ºC, *Ba*AA10 + Cu^{2+} + Chitin = 68.7 ºC. Following the initial melting of the protein the fluorescence is observed to decrease again at higher temperatures. This is likely the result of protein aggregation following protein unfolding. As the exposed hydrophobic residues come together during aggregation, the SYPROorange dye is displaced resulting in a loss of fluorescence.

Dalton Transactions Accepted Manuscript

Please do not adjust margins

View Article Online
DOI: 10.1039/C6DT02793H

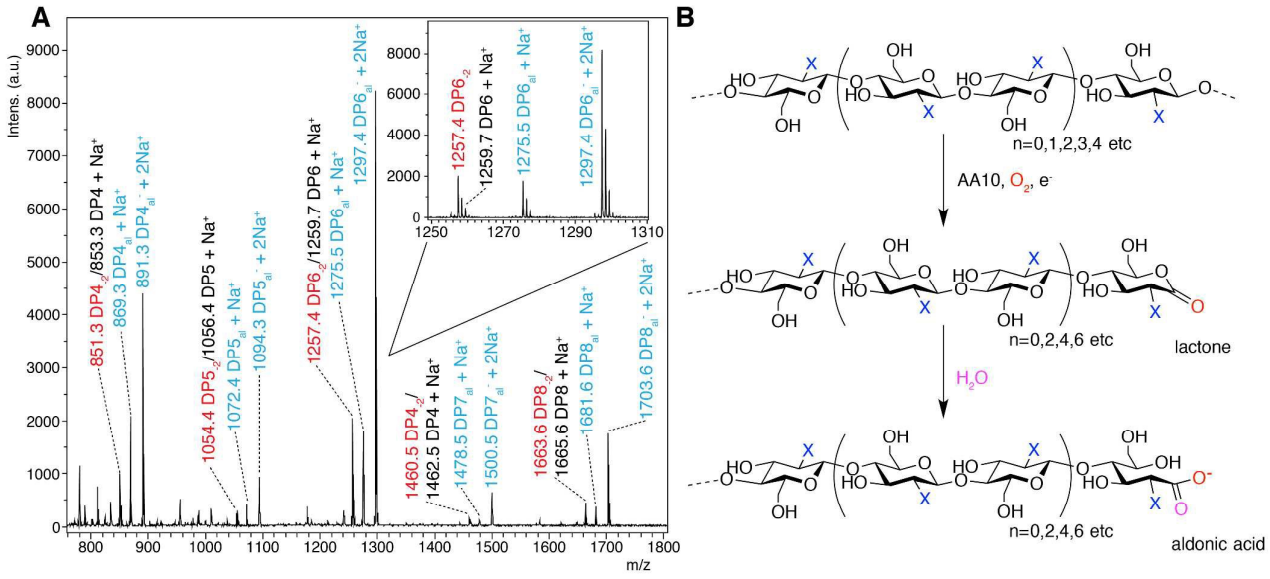

Figure 4. **(A)** MALDI-TOF mass spectrometry analysis of the action of *Ba*AA10 on β-chitin from squid pen. The spectrum shows varying degrees of polymerisation detected as products, with DPn indicating native oligosaccharides coloured black, DPn_{-2} in red indicating the lactone, and DPn_{al} showing aldonic acids coloured blue. A closer look at the individual ion peaks for the DP6 peaks are shown inlaid. **(B)** Schematic diagram showing the AA10 catalysed C1 oxidation of oligosaccharides (X=NHAc, for chitooligosaccharides) to yield lactones and their ring-opened aldonic acids, following the action of an AA10 enzyme in the presence of oxygen and a source of electrons for the reduction of the AA10. n denotes the most common number of repeating units (bound by parentheses) observed for AA10 LPMO reaction products.

Previous work with *Ba*AA10 showed a significant increase in thermal stability for this enzyme in the presence of copper (ΔT_m = 19 °C)[32]. Therefore, this was repeated in the presence of chitin as the potential substrate. The dissociation curves in Figure 3B show that there is indeed a large increase in stability when copper is added to the enzyme (a ΔT_m of 21.6 °C), comparable to published results[32]. There is also a further significant increase in stability when chitin is added to the copper loaded enzyme, with a melting temperature of 68.7 °C, an additional 3.5 degree increase compared to just the enzyme and copper.

*Ba*AA10 is a chitin active LPMO that generates aldonic acid oligosaccharides

That *Ba*AA10 is an active LPMO has been assumed thus far, but experimental confirmation of this activity has been lacking to date. The activity of *Ba*AA10 was, therefore, assessed on a range of substrates, including cellulose (Avicel), α and β chitin, starch, pectin, xylan, mannan, glucomannan, guar gum, locust bean gum and arabinoxylan using MALDI-TOF mass spectrometry. The enzyme showed activity on all chitin sources tested (Figure S2), with the clearest activity observed on β-chitin from squid pen (Figure 4A); the cleanest chitin source which contains very few contaminating chitooligosaccharides. Oxidative degradation products, primarily aldonic acids obtained upon subsequent hydrolysis of the lactones (Figure 4B), formed following oxidation by *Ba*AA10 were clearly resolved. Three main peaks can be seen for each degree of polymerisation, which signify the lactone/Na^+ and the aldonate as both its H^+/Na^+ and $2Na^+$ adducts, each as a result of C1 oxidation. It must be noted that the peaks for the dual Na^+ form are always stronger than the other two for each DP, reflecting the presence of NaCl in the protein buffer prior to dilution in the reaction. Consistent with other work [13, 19, 20], the oxidative degradation products show a strong preference towards the even-numbered products i.e. DP = 4, 6, 8 over the odd-numbered products that are produced (DP = 3, 5, 7 *etc*). The even DP product profiles displayed by chitin active AA10s is likely a result of the stereochemistry of chitin. The two-fold screw axis of individual chitin chains exposes every other C1 carbon of the sugar ring on adjacent faces of the polysaccharide chain. The products observed for *Ba*AA10, therefore, appear to reflect the accessibility of these positions for attack by the enzyme at the surface of the solid substrate. No obvious oxidative degradation products were observed on any of the other polysaccharide substrates tested (results not shown), implying that the main substrate for *Ba*AA10, consistent with its gene locus[33], is chitin.

EPR spectroscopy of *Ba*AA10

Following confirmation that *Ba*AA10 is a chitin active LPMO, X-band EPR spectroscopy of the *Ba*AA10 prepared as described in this work was carried out at 150 K (spectrum shown in red in Figure 5). The resulting spectrum was highly rhombic ($g_x \neq g_y \neq g_z$) with a reduced $|A_z|$ value (125 G) from that expected of a canonical type 2 copper site, although the overall axial envelope of the spectrum shows that the SOMO has $d(x^2-y^2)$ character. The breadth of the peaks also indicated that there was potentially a mixture of species present in solution, as has recently shown by Chaplin et al [34]. As previously discussed, the reduced $|A_z|$ value could arise from mixing of $d(z^2)$ orbital

This journal is © The Royal Society of Chemistry 20xx

Published on 07 September 2016. Downloaded by University of Leeds on 07/09/2016 14:17:33.
Dalton Transactions Accepted Manuscript
Please do not adjust margins

Please do not adjust margins
View Article Online
DOI: 10.1039/C6DT02793H

into the d(x^2–y^2) SOMO as a result of distortion away from axial geometry (see structure discussion below). The spectrum matched that reported previously for *Ba*AA10[32] prepared using periplasmic secretion (Figure 5), showing that the active site geometry of the enzyme prepared in different ways was identical.

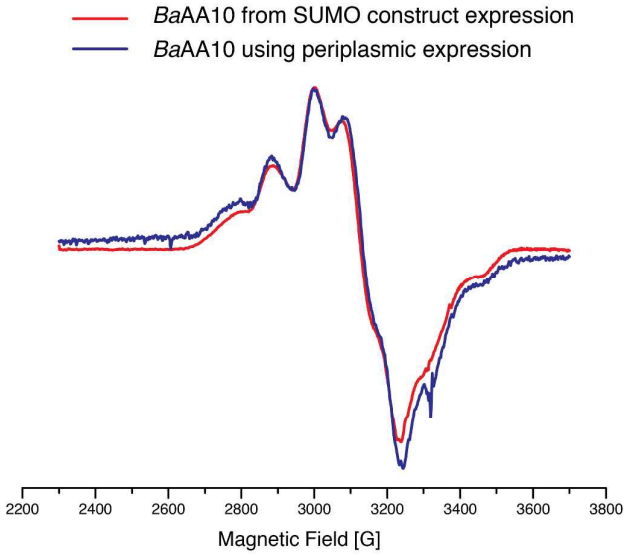

Figure 5. X-band EPR spectra of the original Cu-*Ba*AA10 protein prepared via periplasmic secretion (9 GHz, 155 K, coloured blue)[32], and Cu-*Ba*AA10 produced using a SUMO tag (9 GHz, 150 K, coloured red). The spectra clearly overlay showing the distorted axial coordination geometry is maintained in the SUMO protein purification method described here.

Structure of the Cu(II) form of BaAA10

In order to attain structural information on the active site coordination geometry of the copper in its resting Cu(II) state, a spiral data collection technique was applied to the rod-shaped *Ba*AA10 crystals inspired by the work presented in Gudmundsson *et al*[26] (See Tables S1 and Table 1 for crystallisation and data statistics summaries). As well as using this strategy, it was necessary to reduce the X-ray intensity significantly at only 5% transmission, resulting in fairly weak diffraction data. The auto-processing carried out by xia2 and mosflm at Diamond was not able to process these low intensity data. Careful manual data processing was therefore necessary using XDS[35] and CCP4[36], providing XDS with the likely space group and cell dimensions from previous structure determinations to assist with indexing and data integration. The crystals were of the $P2_1$ form, and contained two molecules in the asymmetric unit. The low intensity nature of the data is reflected in the processing and refinement statistics for these data (Table 1). After refinement of the original $P2_1$ *Ba*AA10 structure with copper, water molecules and flexible loops removed from the model, maps of sufficient quality for model building and refinement were produced containing additional features in the electron density around the copper and regions of the model that had been removed prior to structure solution. The two molecules in AU are essentially identical to one another, with the B chain superposing on the A chain with a root mean square deviation (RMSD) of 0.16 Å over all Cα's in the molecule. The structural analysis performed below uses the A chain unless stated otherwise.

Table 1. Data Collection, Structure Solution and Refinement Statistics.

Diffraction source	Diamond Light Source I04
Space group	$P\ 2_1$
a, *b*, *c* (Å)	34.8, 73.5, 75.5
α, β, γ (°)	90.0, 100.4, 90.0
Mosaicity (°)	0.122
Resolution range (Å)	37.11 – 1.70 (1.73 – 1.70)
Total No. of reflections	136277 (6008)
No. of unique reflections	41043 (2170)
Completeness (%)	99.8 (99.4)
Redundancy	3.3 (2.8)
$\langle I/\sigma(I)\rangle$	5.3 (1.3)[#]
Half-set correlation CC(1/2)	0.985 (0.54)
$R_{p.i.m.}$	0.108 (0.573)
Overall *B* factor from Wilson plot ($Å^2$)	7.3
Refinement Statistics	
Resolution range (Å)	37.11 – 1.70 (1.74 – 1.70)
Completeness (%)	99.7 (99.3)
No. of reflections, working set	38958
No. of reflections, test set	2062
Final R_{cryst}	0.223
Final R_{free}	0.264
No. of non-H atoms	
Protein	2782
Ion	3
Solvent (Ethylene Glycol)	8
Water	282
Total	3075
R.m.s. deviations	
Bonds (Å)	0.014
Angles (°)	1.64
Average B factors (Å2)	
Protein	8.8
Ion	11.3
Solvent (Ethylene Glycol)	21.5
Water	15.2
Ramachandran plot	
Most favoured (%)	97
Allowed (%)	3
PDB entry	5IJU

Values for the outer shell are given in parentheses.

The data collected during this project are necessarily low intensity to avoid photoreduction of the copper. Data were processed to 1.7 Å based on the CC(1/2) > 0.5 criterion – [37]. This statistic has been included in the table. At 1.7 Å CC(1/2) = 0.54 indicating that meaningful data are present at this resolution

The overall protein structure (Figure 6A) is similar to that obtained previously[32], consisting of a core β-sandwich domain with an adjacent helical region at the surface of the enzyme. This flat surface houses the N-terminal active site, and hence provides an extended region for crystalline chitin binding. The Cu(II)-*Ba*AA10 structure determined here reveals the presence of previously unobserved electron density around the copper

Published on 07 September 2016. Downloaded by University of Leeds on 07/09/2016 14:17:33.
Dalton Transactions Accepted Manuscript

Please do not adjust margins

View Article Online
DOI: 10.1039/C6DT02793H

Published on 07 September 2016. Downloaded by University of Leeds on 07/09/2016 14:17:33.

ion resulting from the addition of two water molecules coordinating to the copper (Figure 6B). Neither of the additional water molecules is directly *trans* to the NH_2 nitrogen atom. Rather the two water molecules are distorted away from this position, with H_2O-487 (PDB numbering) and H_2O-412 at 2.18 Å and 1.97 Å from the copper respectively. The shorter distance of the latter Cu-O bond indicates that this water molecule may be deprotonated to the hydroxide. The arrangement of these molecules at the copper centre form an unusual compressed trigonal bipyramidal geometry (bond lengths: $N\varepsilon2_{His125}$-Cu= 2.05 Å, $N\delta1_{His28}$-Cu= 2.01 Å, NH_{His28}-Cu=2.24 Å, $O_{H2O\text{-}412}$-Cu= 1.97 Å and $O_{H2O\text{-}487}$-Cu= 2.18 Å, where the $N\varepsilon2_{His125}$-Cu-$N\delta1_{His28}$ atoms of the histidine brace constitute the axis), as observed for the *Enterococcus faecalis* enzyme (Figure 6C)[26], the O-Cu(II)-NH_2 bond angles for H_2O487 and H_2O412 in Cu(II)-*Ba*AA10 being 131.9° and 128.4° respectively. These data confirm the predicted distorted geometry for the copper centre in this enzyme, as predicted from the high degree of rhombicity observed in our previous original EPR analysis [32].

Detailed comparison of the Cu(I)[32] and Cu(II) structures of *Ba*AA10 reveals only very minor changes in the geometry around the copper as it transitions between oxidation states (Figure S3A). The main and most obvious change is that the copper geometry changes from a T-shaped geometry in its Cu(I) state with only 3 exogenous ligands, to a trigonal bipyramidal geometry in its Cu(II) state with 5 coordinating groups (Figure S3A and B). The bond lengths and angles between the copper and protein derived coordinating atoms change only slightly between the two structures. The two nitrogen ligands provided by the histidine sidechains in the Cu(I) structure form a near linear axis around the copper with the Nε2-Cu-Nδ1 giving a bond angle of 162.6°. This angle straightens slightly in the Cu(II) state to 171.4° when the water molecules are present, resulting in a concomitant shortening of the Cu-NH2 bond to 2.24 Å, but these changes are minor at best. These structures therefore suggest, as is the case for other copper dependent redox enzymes[25], that *Ba*AA10 binds copper such that the metal can transition between redox states without requiring large changes in protein conformation. Such an observation is consistent with the low-temperature reduction of Cu(II)-LPMOs observed by Kjaergaard et al [23]. The reason for the different coordination geometry maintained by chitin active AA10s when compared to other LPMOs remains unclear, but our ability to now obtain Cu(II) complexes for this model system will aid in the delineation of the reaction mechanism utilised by these enzymes during the oxidative deconstruction of chitin.

Conclusions

Taken together, the data presented here confirm *Ba*AA10 is a chitin specific LPMO, which maintains the unusual copper coordination geometry observed for other chitin active AA10s[26, 30, 38]. Using the improved protein purification protocols developed here, we will now be able to investigate the interaction of this enzyme with substrates in greater detail to assist in gaining a molecular level understanding of how this family of enzymes bring about oxidative deconstruction of chitin.

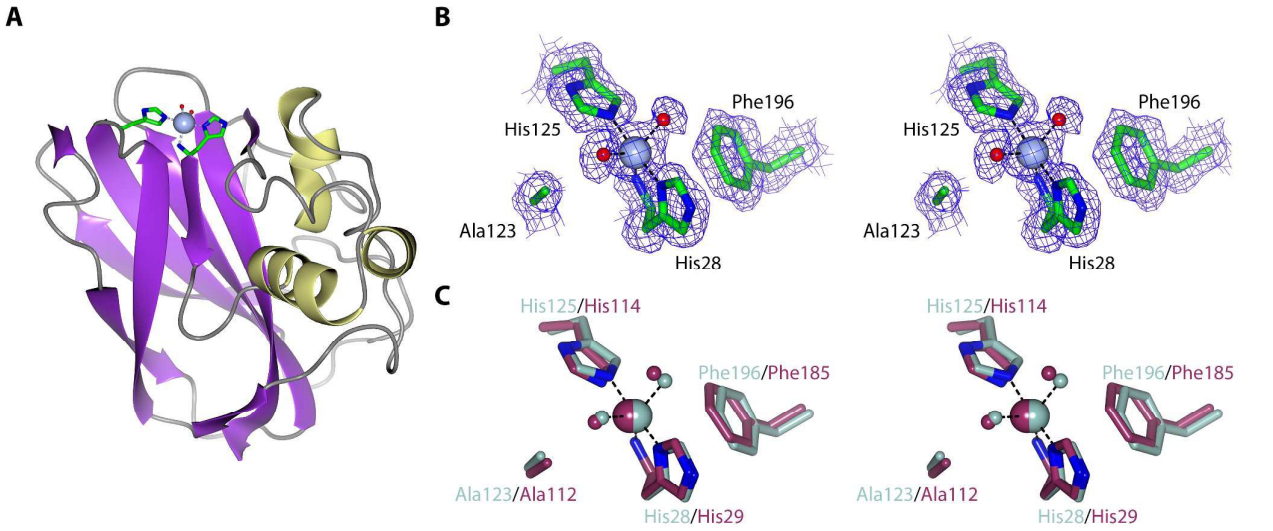

Figure 6. (A) Structural representation of *Ba*AA10, clearly portraying the Cu(II) active site with the familiar 'histidine-brace' and two water molecules. **(B)** Stereo structure of Cu-*Ba*AA10 displaying the $2F_{obs}$-F_{calc} density map at 0.48 e/A^3 (1 σ) contour level, showing the two water molecules coordinated to the copper atom. **(C)** Stereo structure comparison of the AA10 site from *Bacillus amyloliquefaciens* (blue/grey) with that from *Enterococcus faecalis* (purple) [26].

Dalton Transactions Accepted Manuscript

This journal is © The Royal Society of Chemistry 20xx

Please do not adjust margins
View Article Online
DOI: 10.1039/C6DT02793H

Published on 07 September 2016. Downloaded by University of Leeds on 07/09/2016 14:17:33.

Experimental

Re-cloning and overexpression of a SUMO-AA10 construct

The codon-optimised *Ba*AA10 open reading frame used for our previous work[32] was cloned into the Champion pET-SUMO vector (Invitrogen), so that the N-terminal histidine of the protein would be encoded directly after the SUMO protease cleavage site using In-fusion cloning (Clontech). The primers used were: gaacagattggtggtCATGGCTACATCAAGGAACCGG and tacctaagcttgtctTTATTTCGTCAGATTCACGTCGATGAC, where lower case represents the sequence for the overhangs required for insertion into the vector and upper case represents the complementary bases to the protein sequence. pET-SUMO(*Ba*AA10) was then transformed into BL21* *E. coli* cells for overexpression. Cells were grown in LB media supplemented with kanamycin (30 µg/ml), at 37 °C before the temperature was reduced to 16 °C at an OD_{600} of 0.6. *Ba*AA10 production was then induced by the addition of IPTG to a final concentration of 1 mM when the OD_{600} was at 0.8. The cells were left to grow overnight at 16 °C, shaking at 180 rpm, before being harvested by centrifugation at 10 000 *g* for 30 minutes. The cell pellets were resuspended in 5x volumes of Buffer A (50 mM Tris pH 8; 200 mM NaCl; 30 mM Imidazole), sonicated, and cell debris subsequently removed by centrifugation in a Sorvall SS-34 rotor at 38 000 *g* for 20 minutes. The supernatant was then loaded onto a His-trap crude 5 ml Ni column (GE Healthcare) that had been equilibrated in Buffer A. The column was washed with 5 CVs of Buffer A, before applying a gradient from 0 to 100 % Buffer B (50 mM Tris pH 8; 200 mM NaCl; 300 mM Imidazole) over 20 CVs. After combining the fractions containing *Ba*AA10-SUMO, the protein was concentrated and then diluted 10-fold with Buffer A to reduce the imidazole concentration so that the final concentration was ~ 1 mg/ml. DTT was then added to a concentration of 5 mM, along with 10 µg of SUMO protease for every mg of *Ba*AA10-SUMO. The protein was then left incubating at 20 °C overnight with shaking at 10 rpm, before passing through a crude 5 ml Ni column in buffer A. The flow through was collected, and treated with 1 mM EDTA to remove any metals present in the sample. The protein was then concentrated to < 2 ml and loaded onto a 16/60 superdex 75 (GE Healthcare) gel filtration column, which had been equilibrated with GF buffer (20 mM NaOAc pH 5; 250 mM NaCl). 1.6 ml fractions were collected after a void volume of 40 ml and peak fractions containing *Ba*AA10 were combined and concentrated to the required concentrations for experiments and crystallisation.

Displacement ITC to measure binding constant for Cu

Most LPMO Cu binding studies have yielded low nM K_D values, at the limit of conventional ITC. To obtain a more accurate Cu^{2+} binding constant for *Ba*AA10, displacement ITC [39, 40] was carried out using Zn^{2+} as the competing metal. The experiments were performed using an ITC-200 calorimeter (GE Healthcare). All experiments were performed at 298K in 20 mM NaOAc pH 5, 250 mM NaCl. A Zn^{2+} binding titration was first carried out with *Ba*AA10 at 200 µM in the cell and 2 mM $ZnCl_2$ in the syringe. Fitting the data using the Origin 7 (MicroCal) software, generated n = 0.63, K = 1.23 x 10^5 M^{-1}, ΔH = 5424 cal/mol and ΔS = 41.5 cal/mol/K. The displacement experiment was then carried out using 50 µM *Ba*AA10 and 2 mM $ZnCl_2$ in the cell, titrating in $CuCl_2$ at a concentration of 500 µM from the syringe. For each experiment, 38 injections of 1 µL were carried out at 2 min intervals. Copper binding data was then obtained by fitting in Origin 7 (Microcal) using the competitive binding model present in the software, and inserting the Zn^{2+} binding parameters obtained previously into the algorithm. The data presented are from a single experiment.

BaAA10 stability

Thermostability studies were carried out on an Agilent MX3000P qPCR machine. Squid-pen β-chitin (a kind gift from D. Gillet of Mahtani Chitosan), was used as a substrate to test for increased stability, along with cellulose (Avicel) and chitohexaose, and EDTA was used as a control. A further experiment involving the addition of copper to the enzyme (in a stoichiometric amount), followed by the addition of chitin to a copper-loaded sample was also carried out. 15 µl of enzyme:substrate mix was combined with 15 µl of SYPRO orange (1000x diluted from a 5000x concentrated stock solution) in qPCR tubes. The final concentration of *Ba*AA10 was 1.35 mg/ml (~ 65 µM), and the buffer used was 20 mM NaOAc pH 5, 250 mM NaCl. The fluorescence was measured whilst the temperature was increased from 25 to 96 °C, at 1 °C steps every 30 s. 517 and 585 nm were used as the excitation and emission wavelengths, respectively. The resulting melting temperatures were calculated by fitting a sigmoidal curve to the data using the MTSA program for MATLAB[41].

Mass-spectrometry-based activity measurements

The activity of the *Ba*AA10 enzyme was assessed primarily on squid-pen β chitin as it contains fewer contaminating chito-oligosaccharides than chitins obtained from crab or shrimp (α chitins). 1 ml reactions were set up consisting of 2-3 mg/ml of β-chitin from squid (a kind gift from D. Gillet of Mahtani Chitosan), 1 mM ascorbic acid as reducing agent, 1 µM $CuCl_2$ and 1 µM *Ba*AA10. Control reactions were carried out in the absence of enzyme and also in the absence of ascorbic acid. The reactions were carried out in 10 mM ammonium acetate pH 5, and were incubated for ~ 16 h at 30 °C whilst rotating to ensure the solid chitin was constantly being mixed with the reaction solution. After incubation, centrifugation for 1.5 minutes at 13 300 g removed the remaining solid substrate from the mixed suspension. 1 µl of the supernatant was then spotted onto a SCOUT-MTP 384 target plate (Bruker) along with 1 µl of a 10 mg/ml DHB (2,5-dihydroxybenzoic acid) matrix solution, and allowed to dry. An Ultraflex III MALDI-TOF Mass Spectrometer was used to run the samples, using the Bruker flexControl software. Samples were run at 800 shots of 100 Hz laser frequency and a laser power of 40 mW. All spectra were processed and analysed using the Bruker flexAnalysis software.

Dalton Transactions Accepted Manuscript

Please do not adjust margins

View Article Online
DOI: 10.1039/C6DT02793H

Published on 07 September 2016. Downloaded by University of Leeds on 07/09/2016 14:17:33.

3-D structure solution of the Cu(II) form of BaAA10

Crystals grown from 0.1 M MMT pH 4.0; 25 % PEG-1500 were used to generate a seed stock using the seed bead (Hampton Research) technique and 26 % PEG-1500 as the stabilisation solution. This was used to set up a seeding tray on a Douglas Oryx crystallisation robot with ratios of the reservoir solutions, protein and seed bead solutions at 0.25 : 0.30 : 0.05 µl, respectively. The concentration of protein used was 4.7 mg/ml, and $CuCl_2$ was added to the protein in stoichiometric amounts. Rod-shaped crystals were cryo-cooled for data collection by soaking in mother liquor (0.1 M NaOAc p H 5, 20 % PEG-6000, 0.2 M $CaCl_2$) supplemented with 20% ethylene glycol for 30 s before being plunged in liquid nitrogen (See Table S1 for crystallisation summary).

X-ray data collection of the Cu-*Ba*AA10 crystals obtained was carried out at Diamond Light Source (DLS) on beamline I04. Spiral data collection was carried out by running a line scan along the length of the crystal, whilst rotating the crystal by 180°. A 5 µm beam and 5% transmission were used throughout data collection. Data was processed using XDS[35], followed by the Aimless data reduction pipeline on the CCP4i2 software[36] (Table 1). The previous *Ba*AA10 structure (PDB code: 2YOX) was prepared for refinement by removing all water molecules, copper ions and highly flexible loops prior to refinement against the new data to remove model bias. Refinement and subsequent model building was performed using REFMAC5[42] and COOT[43] respectively (Table 1). The final coordinates and structure factors have been deposited in the Protein Data Bank - PDB entry 5IJU.

Acknowledgements

We thank Diamond Light Source for access to beamline I04-1 that contributed to the results presented here. RCG was a BBSRC "White Rose" DTP student, GJD, PHW and GRH are supported by the BBSRC (Grant Codes BB/I014802/1, BB/L000423, BB/L021633/1).

References

1. D. Cannella and H. Jorgensen, *Biotechnology and bioengineering*, 2014, **111**, 59-68.
2. S. J. Horn, G. Vaaje-Kolstad, B. Westereng and V. G. Eijsink, *Biotechnol Biofuels*, 2012, **5**, 45.
3. A. Levasseur, E. Drula, V. Lombard, P. M. Coutinho and B. Henrissat, *Biotechnol Biofuels*, 2013, **6**, 41.
4. G. R. Hemsworth, B. Henrissat, G. J. Davies and P. H. Walton, *Nature chemical biology*, 2014, **10**, 122-126.
5. V. V. Vu, W. T. Beeson, E. A. Span, E. R. Farquhar and M. A. Marletta, *Proc Natl Acad Sci U S A*, 2014, **111**, 13822-13827.
6. L. Lo Leggio, T. J. Simmons, J. C. Poulsen, K. E. Frandsen, G. R. Hemsworth, M. A. Stringer, P. von Freiesleben, M. Tovborg, K. S. Johansen, L. De Maria, P. V. Harris, C. L. Soong, P. Dupree, T. Tryfona, N. Lenfant, B. Henrissat, G. J. Davies and P. H. Walton, *Nature communications*, 2015, **6**, 5961.
7. G. R. Hemsworth, G. J. Davies and P. H. Walton, *Current opinion in structural biology*, 2013, **23**, 660-668.
8. G. R. Hemsworth, E. M. Johnston, G. J. Davies and P. H. Walton, *Trends Biotechnol*, 2015, **33**, 747-761.
9. W. T. Beeson, V. V. Vu, E. A. Span, C. M. Phillips and M. A. Marletta, *Annu Rev Biochem*, 2015, **84**, 923-946.
10. E. A. Span and M. A. Marletta, *Current opinion in structural biology*, 2015, **35**, 93-99.
11. G. Courtade, R. Wimmer, A. K. Rohr, M. Preims, A. K. Felice, M. Dimarogona, G. Vaaje-Kolstad, M. Sorlie, M. Sandgren, R. Ludwig, V. G. Eijsink and F. L. Aachmann, *Proc Natl Acad Sci U S A*, 2016, **113**, 5922-5927.
12. K. E. Frandsen, T. J. Simmons, P. Dupree, J. C. Poulsen, G. R. Hemsworth, L. Ciano, E. M. Johnston, M. Tovborg, K. S. Johansen, P. von Freiesleben, L. Marmuse, S. Fort, S. Cottaz, H. Driguez, B. Henrissat, N. Lenfant, F. Tuna, A. Baldansuren, G. J. Davies, L. Lo Leggio and P. H. Walton, *Nature chemical biology*, 2016, **12**, 298-303.
13. G. Vaaje-Kolstad, B. Westereng, S. J. Horn, Z. Liu, H. Zhai, M. Sorlie and V. G. Eijsink, *Science*, 2010, **330**, 219-222.
14. R. J. Quinlan, M. D. Sweeney, L. Lo Leggio, H. Otten, J. C. Poulsen, K. S. Johansen, K. B. Krogh, C. I. Jorgensen, M. Tovborg, A. Anthonsen, T. Tryfona, C. P. Walter, P. Dupree, F. Xu, G. J. Davies and P. H. Walton, *Proc Natl Acad Sci U S A*, 2011, **108**, 15079-15084.
15. J. A. Langston, T. Shaghasi, E. Abbate, F. Xu, E. Vlasenko and M. D. Sweeney, *Appl Environ Microbiol*, 2011, **77**, 7007-7015.
16. C. M. Phillips, W. T. Beeson, J. H. Cate and M. A. Marletta, *ACS chemical biology*, 2011, **6**, 1399-1406.
17. T. C. Tan, D. Kracher, R. Gandini, C. Sygmund, R. Kittl, D. Haltrich, B. M. Hallberg, R. Ludwig and C. Divne, *Nature communications*, 2015, **6**, 7542.
18. T. Isaksen, B. Westereng, F. L. Aachmann, J. W. Agger, D. Kracher, R. Kittl, R. Ludwig, D. Haltrich, V. G. Eijsink and S. J. Horn, *The Journal of biological chemistry*, 2014, **289**, 2632-2642.
19. F. L. Aachmann, M. Sorlie, G. Skjak-Braek, V. G. Eijsink and G. Vaaje-Kolstad, *Proc Natl Acad Sci U S A*, 2012, **109**, 18779-18784.
20. G. Vaaje-Kolstad, S. J. Horn, M. Sorlie and V. G. Eijsink, *The FEBS journal*, 2013, **280**, 3028-3049.
21. M. Bey, S. Zhou, L. Poidevin, B. Henrissat, P. M. Coutinho, J. G. Berrin and J. C. Sigoillot, *Appl Environ Microbiol*, 2013, **79**, 488-496.
22. M. Wu, G. T. Beckham, A. M. Larsson, T. Ishida, S. Kim, C. M. Payne, M. E. Himmel, M. F. Crowley, S. J. Horn, B. Westereng, K. Igarashi, M. Samejima, J. Stahlberg, V. G. Eijsink and M. Sandgren, *The Journal of biological chemistry*, 2013, **288**, 12828-12839.
23. C. H. Kjaergaard, M. F. Qayyum, S. D. Wong, F. Xu, G. R. Hemsworth, D. J. Walton, N. A. Young, G. J. Davies, P. H. Walton, K. S. Johansen, K. O. Hodgson, B. Hedman and E. I. Solomon, *Proc Natl Acad Sci U S A*, 2014, **111**, 8797-8802.
24. W. T. Beeson, C. M. Phillips, J. H. Cate and M. A. Marletta, *Journal of the American Chemical Society*, 2012, **134**, 890-892.
25. E. I. Solomon, D. E. Heppner, E. M. Johnston, J. W. Ginsbach, J. Cirera, M. Qayyum, M. T. Kieber-Emmons, C. H. Kjaergaard, R. G. Hadt and L. Tian, *Chem Rev*, 2014, **114**, 3659-3853.

Dalton Transactions Accepted Manuscript

This journal is © The Royal Society of Chemistry 20xx

Please do not adjust margins
View Article Online
DOI: 10.1039/C6DT02793H

26. M. Gudmundsson, S. Kim, M. Wu, T. Ishida, M. H. Momeni, G. Vaaje-Kolstad, D. Lundberg, A. Royant, J. Stahlberg, V. G. Eijsink, G. T. Beckham and M. Sandgren, *The Journal of biological chemistry*, 2014, **289**, 18782-18792.
27. S. Kim, J. Stahlberg, M. Sandgren, R. S. Paton and G. T. Beckham, *Proc Natl Acad Sci U S A*, 2014, **111**, 149-154.
28. J. Y. Lee and K. D. Karlin, *Current opinion in chemical biology*, 2015, **25**, 184-193.
29. Y. S. Nakagawa, M. Kudo, J. S. Loose, T. Ishikawa, K. Totani, V. G. Eijsink and G. Vaaje-Kolstad, *The FEBS journal*, 2015, **282**, 1065-1079.
30. Z. Forsberg, A. K. Rohr, S. Mekasha, K. K. Andersson, V. G. Eijsink, G. Vaaje-Kolstad and M. Sorlie, *Biochemistry*, 2014, **53**, 1647-1656.
31. Z. Forsberg, A. K. Mackenzie, M. Sorlie, A. K. Rohr, R. Helland, A. S. Arvai, G. Vaaje-Kolstad and V. G. Eijsink, *Proc Natl Acad Sci U S A*, 2014, **111**, 8446-8451.
32. G. R. Hemsworth, E. J. Taylor, R. Q. Kim, R. C. Gregory, S. J. Lewis, J. P. Turkenburg, A. Parkin, G. J. Davies and P. H. Walton, *Journal of the American Chemical Society*, 2013, **135**, 6069-6077.
33. H. H. Chu, V. Hoang, J. Hofemeister and H. Schrempf, *Microbiology*, 2001, **147**, 1793-1803.
34. A. K. Chaplin, M. T. Wilson, M. A. Hough, D. A. Svistunenko, G. R. Hemsworth, P. H. Walton, E. Vijgenboom and J. A. Worrall, *The Journal of biological chemistry*, 2016, DOI: 10.1074/jbc.M116.722447.
35. W. Kabsch, *Acta crystallographica. Section D, Biological crystallography*, 2010, **66**, 125-132.
36. M. D. Winn, C. C. Ballard, K. D. Cowtan, E. J. Dodson, P. Emsley, P. R. Evans, R. M. Keegan, E. B. Krissinel, A. G. Leslie, A. McCoy, S. J. McNicholas, G. N. Murshudov, N. S. Pannu, E. A. Potterton, H. R. Powell, R. J. Read, A. Vagin and K. S. Wilson, *Acta crystallographica. Section D, Biological crystallography*, 2011, **67**, 235-242.
37. P. A. Karplus and K. Diederichs, *Science*, 2012, **336**, 1030-1033.
38. Z. Forsberg, C. E. Nelson, B. Dalhus, S. Mekasha, J. S. Loose, L. I. Crouch, A. K. Rohr, J. G. Gardner, V. G. Eijsink and G. Vaaje-Kolstad, *The Journal of biological chemistry*, 2016, DOI: 10.1074/jbc.M115.700161.
39. Y. Liang, *Acta Biochim Biophys Sin (Shanghai)*, 2008, **40**, 565-576.
40. A. Velazquez-Campoy and E. Freire, *Nat Protoc*, 2006, **1**, 186-191.
41. M. N. Schulz, J. Landstrom and R. E. Hubbard, *Analytical biochemistry*, 2013, **433**, 43-47.
42. G. N. Murshudov, A. A. Vagin and E. J. Dodson, *Acta crystallographica. Section D, Biological crystallography*, 1997, **53**, 240-255.
43. P. Emsley, B. Lohkamp, W. G. Scott and K. Cowtan, *Acta crystallographica. Section D, Biological crystallography*, 2010, **66**, 486-501.

Published on 07 September 2016. Downloaded by University of Leeds on 07/09/2016 14:17:33.
Dalton Transactions Accepted Manuscript

Please do not adjust margins

View Article Online
DOI: 10.1039/C6DT02793H

Published on 07 September 2016. Downloaded by University of Leeds on 07/09/2016 14:17:33.

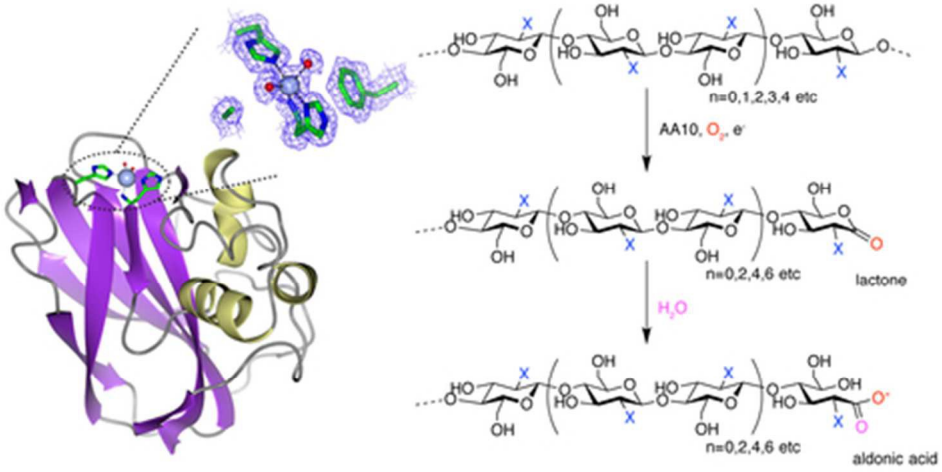

39x19mm (300 x 300 DPI)

Dalton Transactions Accepted Manuscript